JOURNAL OF APPLIED ELECTROCHEMISTRY 24 (1994) 390–395

Thermodynamic descriptions of oxygen redistribution in a nuclear fuel pellet: Heat of transport of oxygen in mixed conductors

M. KAMATA, T. ESAKA

Department of Materials Science, Faculty of Engineering, Tottori University, Koyama, Tottori 680, Japan

Received 27 January 1993; revised 12 September 1993

Transport processes in a mixed conductor (e.g. a UO_2 pellet) are rigorously described by using an irreversible thermodynamic approach and a re-evaluation of the effect of thermoelectric power is carried out. The results indicate that the oxygen redistribution can be interpreted as an electrochemical mass transport phenomenon caused by thermoelectric power. The validity of this interpretation is confirmed using experimental results from other sources.

List of symbols

a_i	activity of component i (–)
c_i	concentration of component i (mol cm^{-3})
D_i	diffusion coefficient (cm^2 s^{-1})
F	Faraday constant (96 500 C mol^{-1})
I	current density (A cm^{-2})
J_i	mass flux (mol cm^{-2} s^{-1})
J_q	heat flux (J cm^{-2} s^{-1})
Q^*	heat of transport (J mol^{-1})
Q_i	(in Fig. 6) heat of transport of oxygen interstitial (kcal mol^{-1})
Q_v	(in Fig. 6) heat of transport of oxygen vacancy (kcal mol^{-1})
R	gas constant (8.3143 J mol^{-1} K^{-1})
$\hat{S}$	Eastman entropy (J K^{-1} mol^{-1})
$S'(Q)$	Peltier entropy (J K^{-1} mol^{-1})
S^*	transported entropy (J K^{-1} mol^{-1})
s	partial molar entropy (J K^{-1} mol^{-1})
T	absolute temperature (K)
t_e	transport number of electron (–)
t_i	transport number of ion (–)
V_U	(in Fig. 6) uranium valency (–)
V_{Pu}	(in Fig. 6) plutonium valency (–)
x_i	molar ratio of component i (–)

Greek symbols

ϵ_O	initial thermoelectric power of an imaginary sample (V K^{-1})
ϵ^{obs}	initial thermoelectric power of a mixed conductor (V K^{-1})
μ_{iT}	chemical potential (J mol^{-1})
σ_e	electronic conductivity (S cm^{-1})
σ_i	ionic conductivity (S cm^{-1})
Φ^{obs}	electrode potential in a mixed conductor (V)

1. Introduction

Fuel pellets used in nuclear reactors are made of UO_2 or mixtures of UO_2 and PuO_2. Their shapes are illustrated in Fig. 1(a). These pellets are packed within a zircaloy cladding as shown in Fig. 1(b) and loaded into the reactor. It is widely known that oxygen redistribution is caused in these fuel pellets while they are irradiated in a reactor [1, 2]. If a large amount of oxygen is redistributed and uniformity of composition is lost, uniformity of thermal and/or mechanical properties might also be lost, which in turn may reduce the thermal and/or mechanical stability of the pellet. Also, as the inner wall of the cladding is attacked by oxygen emanating from the pellets, the behaviour of oxygen in a pellet is important from the viewpoint of the corrosion failure of the zircaloy cladding.

Previously several mechanisms have been proposed for oxygen redistribution. At present, thermal diffusion in the solid phase is widely accepted [3]. Sari has pointed out the contribution of thermoelectric effects to this phenomenon, but recently he presented experimental results which indicate that the contribution of the thermoelectric power is relatively small [4].

A UO_2 pellet is an ionic and electronic mixed conductor and thermodynamic descriptions of transport processes in mixed conductors are not identical to those in pure ionic or pure electronic conductors. For example, although the thermoelectric power is believed to be small when the measured thermoelectric power is small, this is not always true for mixed conductors. However, Sari, as well as other workers, used 'heat of transport' to describe the magnitude of thermal diffusion without paying much attention to the rigorous definition or the physical meaning of 'heat of transport' in the mixed conductor. Thus, there exist some ambiguities in their conclusions and this ambiguity must be resolved.

The purpose of this work is to present thermodynamic descriptions of oxygen transport processes in mixed conductors, and to demonstrate that

0021-891X 1994 Chapman & Hall

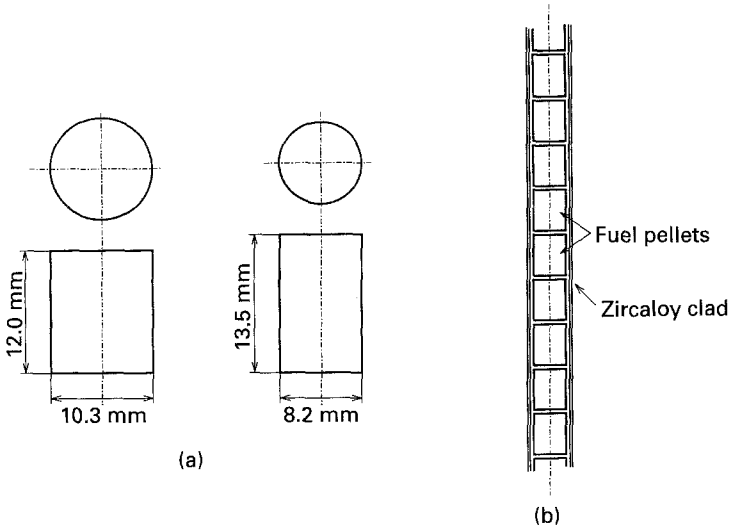

Fig. 1. Nuclear fuel pellets. (a) Left: those used in BWR (boiling water reactor); right: those used in PWR (pressurized water reactor) (b) pellets in a clad.

so-called thermal diffusion in mixed conductors can be interpreted as an electrochemical mass flux caused by thermoelectric power.

2. Theory

Suppose that the oxide fuel is composed of two *thermodynamic components*, MO_2 and MO_3 (M = U or U + Pu) in case it is hyperstoichiometric. The 'thermodynamic components' are the neutral chemical species which are needed to describe the system, and therefore, the chemical form of MO_3 need not be stable or really exist. (It should be noted here that the choice of the thermodynamic components is not unique. For example, the system considered may be described as MO_2–O (excess O in MO_2 system). In the case of the fuel being hypostoichiometric, all descriptions below are still valid if MO_3 is substituted by MO.

Although the real oxide system or the fuel pellet is continuous, it is to be treated as an assembly of small subsystems as shown in Fig. 2 and local equilibrium is assumed in each subsystem. This means that if the temperatures of both ends of the whole system are T_1 and T_2, and the temperature profile between them is continuous, as illustrated by the dotted line in Fig. 2, the temperature of each subsystem is assumed to be constant as illustrated by the solid lines.

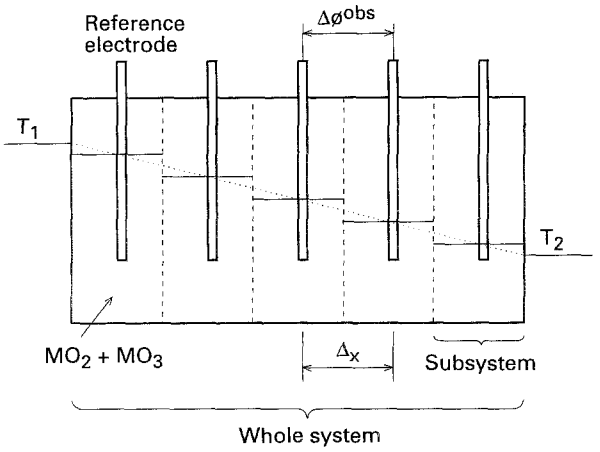

Fig. 2. Schematic illustration of local equilibrium in a continuous system.

According to Førland [5], the fluxes of heat, mass (MO_3) and electric charge are presented as follows. (Here, MO_2 is chosen as the frame of reference.)

$$J_{q'} = -Y_{q'q'}\nabla \ln T - Y_{q'i}\nabla\mu_{iT} - Y_{q'Q}\nabla\Phi^{obs} \quad (1)$$

$$J_i = -Y_{iq'}\nabla \ln T - Y_{ii}\nabla\mu_{iT} - Y_{iQ}\nabla\Phi^{obs} \quad (2)$$

$$I = -Y_{Qq'}\nabla \ln T - Y_{Qi}\nabla\mu_{iT} - Y_{QQ}\nabla\Phi^{obs} \quad (3)$$

where ∇ denotes the difference of intensive variables between two adjacent subsystems for unit distance apart. $\nabla\mu_{iT}$ is the gradient of chemical potential of component i (or MO_3) based on the gradient of its concentration or the pressure, and Φ^{obs} is the electric potential which can be measured using a reference electrode* inserted in the pellet. The potential of the reference electrode is determined by the reaction; $M^{4+} = M^{6+} + 2e^-$.

Since oxide fuel is an ionic and electronic mixed conductor, there exist two paths for charge transfer through the system. In order to clarify the effect of thermoelectric power with simple expressions, the electronic current is treated as a short-circuited current passing through the external circuit as shown in Fig. 3. Therefore the external current, I_e, always exists even when the real circuit between two reference electrodes is open.

$$I_e = -\sigma_e\nabla\Phi^{obs} \quad (4)$$

where σ_e presents the electronic conductivity of the

* Materials of reference electrodes are arbitrary as far as they are nonreactive (eg. Au, Pt).
O_2 (gas) is not supposed to take part in the electrode reaction.

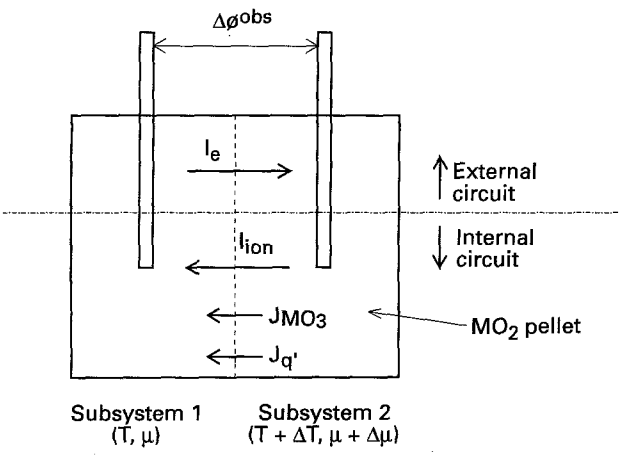

Fig. 3. Transfer of heat, mass and electric charge between two adjacent subsystems.

pellet. Although Y_{QQ} presents the total conductivity of the pellet in usual procedures, where both ionic and electronic currents are treated as the inner current, Y_{QQ} does not include the electronic conductivity here because the electronic current is now treated as the external one.

Using Equation 4 and the relation $I = -I_e$ in Equation 3 gives

$$\sigma_e \nabla \Phi^{obs} = -Y_{Qq'} \nabla \ln T - Y_{Qi} \nabla \mu_{iT} - Y_{QQ} \nabla \Phi^{obs} \quad (5)$$

Thus $\nabla \Phi^{obs}$ is given by

$$\nabla \Phi^{obs} = \frac{-Y_{Qq'} \nabla \ln T - Y_{Qi} \nabla \mu_{iT}}{Y_{QQ} + \sigma_e} \quad (6)$$

and by substituting Equation 6 into Equation 2, the mass flux of MO_3 may be expressed as

$$\begin{aligned} J_i = & - Y_{iq'} \nabla \ln T - Y_{ii} \nabla \mu_{iT} \\ & - Y_{iQ} \left(\frac{-Y_{Qq'} \nabla \ln T - Y_{Qi} \nabla \mu_{iT}}{Y_{QQ} + \sigma_e} \right) \\ = & - Y_{iq'} - \left(\frac{[Y_{iQ} Y_{Qq'}]}{Y_{QQ} + \sigma_e} \right) \nabla \ln T \\ & - Y_{ii} - \left(\frac{[Y_{iQ} Y_{Qi}]}{Y_{QQ} + \sigma_e} \right) \nabla \mu_{iT} \end{aligned} \quad (7)$$

From Equation 6, on the other hand, the initial thermoelectric power measured under the condition $\nabla \mu_{iT} = 0$ is expressed as

$$\epsilon^{obs} = \frac{d\Phi^{obs}}{dT} = -\frac{1}{T} \left(\frac{Y_{Qq'}}{Y_{QQ} + \sigma_e} \right) \quad (8)$$

Therefore, Equation 7 can be rewritten as follows by using ϵ^{obs}:

$$\begin{aligned} J_i = & - (Y_{iq'} - Y_{iQ} T \epsilon^{obs}) \nabla \ln T \\ & - Y_{ii} - \left(\frac{[Y_{iQ} Y_{Qi}]}{Y_{QQ} + \sigma_e} \right) \nabla \mu_{iT} \end{aligned} \quad (9)$$

The first term in the right hand side of Equation 9 has been previously treated as a mass flux of thermal diffusion.

Since the mass flux is generally presented by the following equation using a heat of transport, Q^*, and a diffusion coefficient D_i (see Appendix)

$$J_i = -D_i \left[\left(\frac{Q^* c_i}{RT} \right) \left(\frac{d \ln T}{dx} \right) + \frac{dc_i}{dx} \right] \quad (10)$$

the coefficient of $\nabla \ln T$ in Equation 9 corresponds to the heat of transport. The effect of thermoelectric power on the heat of transport seems to be small when the measured thermoelectric power, ϵ^{obs}, is small. Sari pointed out that the effect of thermoelectric power on the oxygen redistribution is small because the measured value was small. However, to evaluate the effect of thermoelectric power, comparison of Y_{iq}, with ϵ^{obs} is inadequate. It is more important to clarify the physical meaning of the first term in the right hand side of Equation 9.

Here an imaginary sample is assumed which has no electronic conductivity but has the same phenomenological coefficients as Equation 1. As for this imaginary sample, $\sigma_e = 0$ is valid in Equation 5, and therefore the following equation is valid:

$$\nabla \phi^{obs} = -\left(\frac{Y_{Qq'}}{Y_{QQ}} \right) \nabla \ln T - \left(\frac{Y_{Qi}}{Y_{QQ}} \right) \nabla \mu_{iT} \quad (11)$$

Substituting Equation 11 into Equation 2, the mass flux of MO_3, J_i, in this imaginary sample can be written as

$$\begin{aligned} J_{i'} = & - \left(Y_{iq'} - \frac{Y_{iQ} Y_{Qq'}}{Y_{QQ}} \right) \nabla \ln T \\ & - \left(Y_{ii} - \frac{Y_{iQ} Y_{Qi}}{Y_{QQ}} \right) \nabla \mu_{iT} \end{aligned} \quad (12)$$

Subtracting Equation 12 from Equation 7, the difference between the mass flux in a mixed conductor and that in an ionic conductor (imaginary sample) can be expressed as follows:

$$\begin{aligned} \Delta J_i = & J_i - J_{i'} \\ = & Y_{iQ} Y_{Qq'} \left(\frac{1}{\sigma_e + Y_{QQ}} - \frac{1}{Y_{QQ}} \right) \nabla \ln T \\ & + Y_{iQ} Y_{Qi} \left(\frac{1}{\sigma_e + Y_{QQ}} - \frac{1}{Y_{QQ}} \right) \nabla \mu_{iT} \\ = & \frac{Y_{iQ} Y_{Qq'}}{Y_{QQ}} \left(\frac{-\sigma_e}{\sigma_e + Y_{QQ}} \right) \nabla \ln T \\ & + \frac{Y_{iQ} Y_{Qi}}{Y_{QQ}} \left(\frac{-\sigma_e}{\sigma_e + Y_{QQ}} \right) \nabla \mu_{iT} \end{aligned} \quad (13)$$

If the reaction resistance is negligibly small, Y_{QQ} is equal to the ionic conductivity of the sample, which is expressed as σ_{ion}. Therefore, Equation 13 is rewritten as follows by using the electron transport number: $t_e = \sigma_e / (\sigma_e + \sigma_{ion})$

$$\Delta J_i = -\left(\frac{Y_{iQ} Y_{Qq'}}{Y_{QQ}} \right) t_e \nabla \ln T - \left(\frac{Y_{iQ} Y_{Qi}}{Y_{QQ}} \right) t_e \nabla \mu_{iT} \quad (14)$$

From Equation 11, the initial thermoelectric power of an imaginary sample, ϵ_0, is

$$\epsilon_0 = -\frac{1}{T}\left(\frac{Y_{Qq'}}{Y_{QQ}}\right) \tag{15}$$

As for Y_{iq} and $Y_{QQ'}$ the following equation is valid:

$$\left.\frac{J_i}{I}\right|_{\substack{\nabla T=0\\ \nabla\mu=0}} = \frac{Y_{iQ}}{Y_{QQ}} = -\frac{1}{2F} \tag{16}$$

Since Y_{QQ} is equal to σ_{ion}, by using Equation 16 with Onsager's reciprocal relation; $Y_{iQ} = Y_{Qi}$,

$$Y_{iQ} = Y_{Qi} = \frac{-\sigma_{ion}}{2F} \tag{17}$$

Thus, Equation 14 can be rewritten as

$$\Delta J_i = -\left(\frac{\sigma_{ion}\epsilon_0 t_e}{2F}\right)\nabla T - \left(\frac{\sigma_{ion} t_e}{(2F)^2}\right)\nabla\mu_{iT} \tag{18}$$

Here it is assumed that the mobility of O^{2-} is far larger than that of the other ions in the imaginary sample. Thus it is expected that $J_{i'}$, given by Equation 12, is much smaller than J_i (Eq. (17)) with respect to all terms, because of the restriction of electroneutrality.

Thus $\Delta J_i = J_i$ and

$$J_i = -\left(\frac{\sigma_{ion}\epsilon_0 t_e}{2F}\right)\nabla T - \left(\frac{\sigma_{ion} t_e}{(2F)^2}\right)\nabla\mu_{iT} \tag{19}$$

is approximately valid.

If the system is considered to be ideal, the relation $\nabla\mu_{iT} = (RT/c_i)\nabla c_i$ is valid. Therefore the following relations are obtained by comparing Equation 10 with Equation 19.

$$D_i = \frac{\sigma_{ion} t_e RT}{(2F)^2 c_i} \tag{20}$$

$$Q^* = 2F\epsilon_0 T \tag{21}$$

Therefore, in the case of mixed conductors, the so-called heat of transport is given by the thermoelectric power of the (imaginary) ionic conductor.

On the other hand, as shown in Fig. 4 (an equivalent circuit of two adjacent subsystems) the current, I, of the circuit is given by

$$I = \epsilon_0 \nabla T\left(\frac{1}{\sigma_{ion}} + \frac{1}{\sigma_e}\right)^{-1} \tag{22}$$

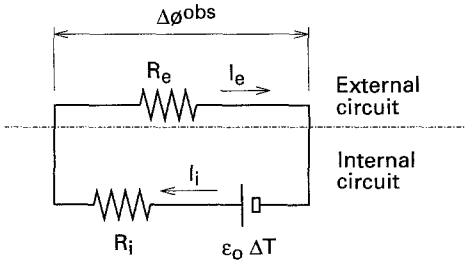

Fig. 4. Equivalent circuit to present the transfer of charge between two adjacent subsystems. ($R_e = l/\sigma_e S$, $R_i = l/\sigma_i S$, l (cm): distance between two adjacent subsystems, S (cm^2): cross section of a subsystem).

The first term in the right hand side of Equation 19, which has been interpreted as the thermal diffusion so far, can be rewritten as follows by using this current I.

$$-\left(\frac{\sigma_{ion}\epsilon_0 t_e}{2F}\right)\nabla T = \frac{1}{2F}\epsilon_0\nabla T\left(\frac{1}{\sigma_{ion}} + \frac{1}{\sigma_e}\right)^{-1} = \frac{I}{2F} \tag{23}$$

The above equation means that this flux can be interpreted as an electrochemical one.

As for the observed potential gradient, this can be written as follows by using the thermoelectric power of the imaginary sample.

$$\nabla\Phi^{obs} = (1/\sigma_e)I = t_i\epsilon_0\nabla T \tag{24}$$

When the measured value of $\nabla\Phi^{obs}$ is small due to small thermoelectric power, ϵ_0, Sari's suggestion that the effect of thermoelectric power is small is reasonable, as indicated in Equations 19 and 24. But when measured $\nabla\Phi^{obs}$ is small due to small t_i, $t_e(= 1 - t_i)$ is close to unity. There is no theoretical limit to the mass flux caused by thermoelectric power.

3. Evaluation of mass flux by using electrochemical mechanism

When Equation 19 was derived, $J_i \gg J_i'$ was assumed. In order to confirm the validity of this assumption, the mass flux of oxygen in a fuel pellet is calculated using Equation 19.

Numerical values used in the calculations are as shown in Table 1. The temperature gradient listed in this table is a typical value observed in a fuel pellet under operation. The thermoelectric power of the imaginary sample, ϵ_0, could be measured by using a thermocell composed of a fuel pellet and some ionic conductor which blocks the flow of electrons, but no data is currently available. Also, the value of ϵ_0 depends on the composition of the sample, as explained in the following Section. Therefore it is not rigorous to assume some constant value for this parameter, but, as a rough approximation, the value listed in Table I was assumed by considering the measured values in ZrO_2 and some molten salt systems [6, 7]. As for conductivities, no data exist for electronic and ionic conductivities of the pellet separately. Extrapolated values of $(U_{0.7}Y_{0.3})O_2$ at 1000° C were adopted [8].

Using these values with Equation 19, J_i was calculated to be $J_i = 5.0 \times 10^{-7}$ mol cm^{-2} s^{-1}. This calcu-

Table 1. Numerical values used to calculate oxygen flux in a fuel pellet

Temperature gradient	2500 K cm^{-1}
Thermoelectric power	0.1 mV K^{-1}
Ionic conductivity	0.4 S cm^{-1}*
Electronic conductivity	9.5 S cm^{-1}*

* Extrapolated values at 1000° C

lated value is so large that nearly a quarter of the oxygen atoms move from one side to the other side within a few hours for a 1 cm thickness. (It should be noted here that a large gradient of composition cannot exist in the steady state because of concentration diffusion.) Since the grounds of the numerical values in Table 1 are not rigorous, the accuracy of the obtained value is rather limited. But it has been made clear that so-called thermal diffusion, which can be interpreted as an electrochemical mass flux, can be evaluated using electrochemical parameters. Since the order of the value obtained is adequate to explain the time which Sari needed to obtain steady state in his experiments [2], Equation 19 or the assumption $J_i \gg J_i'$ is considered to be valid.

4. Composition dependence of ε_0

In order to know how the thermoelectric power of the imaginary sample (ionic conductor) depends on the composition, the entropy change in the electrode region caused by transfer of unit charge must be calculated. It is assumed that the temperature of this region is maintained constant by a heat reservoir.

When one faraday of positive electric charge is transferred through the ionic conductor from right to left as shown in Fig. 5, 1/2 mol MO_2 is consumed and 1/2 mol MO_3 is created at the right hand side electrode. Therefore the entropy change due to the electrode reaction in this region can be presented as follows by using the partial molar entropy of each species; s_{MO_3}, s_{MO_2}.

$$\tfrac{1}{2}(s_{MO_3} - s_{MO_2}) = \tfrac{1}{2}[(s^0_{MO_3} - s^0_{MO_2}) - R\ln(a_{MO_3}/a_{MO_2})] \quad (25)$$

On the other hand, supposing that the entropy carried out from the region by the transfer of electrons through a lead is presented as S_e^* and the entropy carried in with the transfer of O^{2-} is presented as $S^*_{O^{2-}}$, then the Peltier entropy $S'(Q)$, which is the entropy that the right-hand side electrode region absorbs as a heat from the heat reservoir, can be written as,

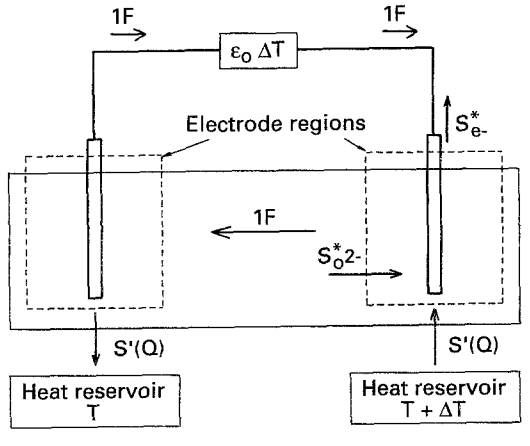

Fig. 5. Entropy balance in an electrode region.

$$S'(Q) = \tfrac{1}{2}[(s^0_{MO_3} - s^0_{MO_2}) - R\ln(a_{MO_3}/a_{MO_2}) - S^*_{O^{2-}} + S^*_e] \quad (26)$$

Since the following relations are available,

$$a_{MO_3} = a_{M^{6+}}a^3_{O^{2-}}$$

$$a_{MO_2} = a_{M^{4+}}a^2_{O^{2-}}$$

$$S^*_{O^{2-}} = (s^0_{O^{2-}} - R\ln a_{O^{2-}}) + \hat{S}_{O^{2-}}$$

Equation 26 may be rewritten as

$$S'(Q) = \tfrac{1}{2}[\{(s^0_{MO_3} - s^0_{MO_2}) - s^0_{O^{2-}} - \hat{S}_{O^{2-}} + S^*_e\} - R\ln(a_{M^{6+}}/a_{M^{4+}})] \quad (27)$$

Within a limited composition region where the molar ratio of MO_3 is small, each term in { } is assumed to be constant and $a_{M^{4+}}$ and $a_{M^{6+}}$ is proportional to $x_{M^{4+}}$ and $x_{M^{6+}}$, respectively. If the sum of the constant terms are expressed as C, the following equation is valid.

$$S'(Q) = \tfrac{1}{2}\{C - R\ln(x_{M^{6+}}/x_{M^{4+}})\} \quad (28)$$

The Peltier entropy $S'(Q)$ and the initial thermoelectric power ϵ_0 may be related by [9]

$$-F\epsilon_0 = S'(Q) \quad (29)$$

Using Equations 28 and 29 the thermoelectric power, ϵ_0, can be expressed as

$$\epsilon_0 = -\frac{1}{2F}[C - R\ln(x_{M^{6+}}/x_{M^{4+}})] \quad (30)$$

In the case of hypostoichiometric composition, the following equation is obtained using a similar procedure:

$$\epsilon_0 = -\frac{1}{2F}[C' - R\ln(x_{M^{4+}}/x_{M^{2+}})\} \quad (31)$$

Equations 30 and 31 imply the following:
(i) For the case of hyperstoichiometric compositions and small nonstoichiometry, $\epsilon_0 < 0$ and ϵ_0 approaches minus infinity as x approaches 0.
(ii) For the case of hypostoichiometric compositions and small nonstoichiometry, $\epsilon_0 > 0$, and ϵ_0 approaches plus infinity as x approaches 0.

From Equation 21 (or $Q^* = -2F\epsilon_0$ in the case of hypostoichiometric composition), the heat of transport decreases to minus infinity as the composition of the sample becomes more stoichiometric. This tendency is in agreement with Sari's experimental work, which is presented in Fig. 6.

The relation between thermoelectric power, which is calculated from the heat of transport in Fig. 6 using Equation 21, and the logarithm of x_{MO_3}/x_{MO_2} or x_{MO_2}/x_{MO} is presented in Fig. 7. Although the deviation of the data in (b) is large, the slopes of both lines are coincident with + (or −) $RT/2F$ within statistical errors according to the least squares method.

It is also made clear by these two figures that the

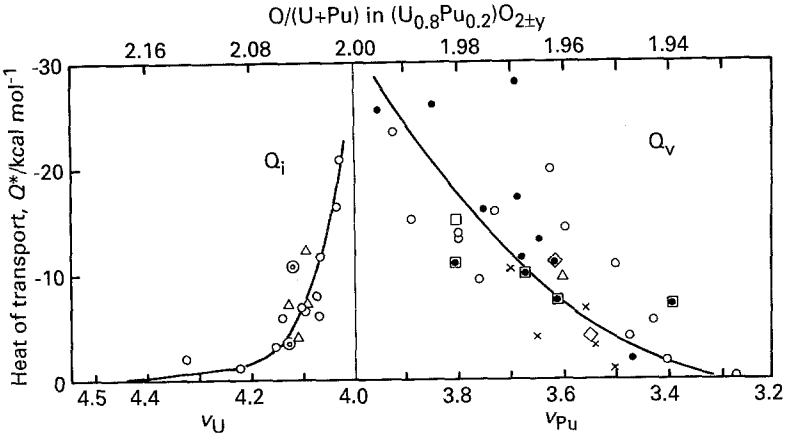

Fig. 6. Heat of transport of oxygen measured by Sari [3]. Values of Sari's work: (○) 15, (△) 20, (+) 30, (×) 40, (□) 50, (◇) 85, (●) 100 mol % plutonium oxide. Values of other workers: (⊙, ⊡) 15 mol % and (◈) 25 mol % plutonium oxide.

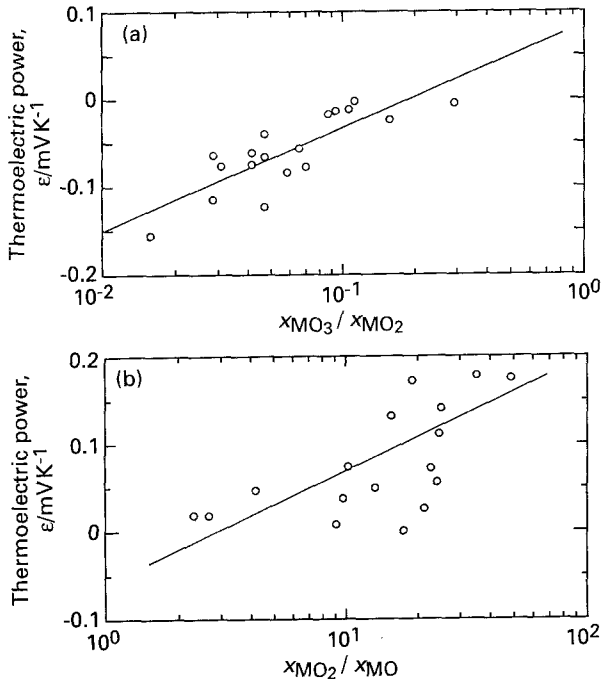

Fig. 7. Thermoelectric power calculated from Sari's data [3]. (a) Hypostoichiometric composition; (b) hyperstoichiometric composition.

absolute value of thermoelectric power assumed in the previous section (cf. Table 1) is reasonable.

5. Conclusions

(i) Transport processes in a mixed conductor are described by using irreversible thermodynamics. In this work, by regarding an electronic current as an external current, the relation between thermoelectric power and heat of transport has been made clear.
(ii) Most of the oxygen flux in an oxide pellet, which is considered to be thermal diffusion, can be interpreted as an electrochemical mass flux caused by thermoelectric power.
(iii) The numerical value of the oxygen flux calculated using electrochemical parameters are roughly coincident with the experimental results from other sources.
(iv) The composition dependence of the measured heat of transport was found to be the same as that of the thermoelectric power.

References

[1] E. A. Aitken, *J. Nucl. Mater.* **30** (1960) 62.
[2] C. Sari and G. Schumacher, *J. Nucl. Mater.* **61** (1976) 192.
[3] C. Sari and G. Schumacher, IAEA-SM-236/25 (1982) 439.
[4] M. Sugisaki, S. Sato and H. Furuya, *J. Nucl. Mater.* **97** (1981) 79.
[5] K. S. Førland, T. Førland and S. K. Ratkje, "Irreversible Thermodynamics, Theory and Applications", Wiley, Chichester (1988) pp. 108–133.
[6] K. Kanamura, S. Yoshioka and Z. Takehara, *J. Electrochem. Soc.* **138** (1991) 2165.
[7] Y. Ito, S. Horikawa, J. Oishi and Y. Ogata, *Electrochim. Acta* **30** (1985) 799.
[8] S. P. S. Badwal and D. J. M. Bevan, *J. Mater. Sci.* **14** (1979) 2353.
[9] M. Kamata, Y. Ito and J. Oishi, *Electrochim. Acta* **33** (1988) 359.

Appendix

According to Førland [5], the heat of transfer, Q^*, is defined by the phenomenological coefficients in Equations 1–3 as follows:

$$Q^* = (J_{q'}/J_i)_{\substack{\nabla \ln T=0 \\ I=0}} = l_{12}/l_{22} \qquad \text{(A1)}$$

where $l_{12} = Y_{iq'} - Y_{iQ}Y_{Qq'}/Y_{QQ}$ and $l_{22} = Y_{ii} - Y_{iQ}Y_{Qi}/Y_{QQ}$.

On the other hand, if we treat the electronic current as the inner current just as other workers do, Equation 2 can be simplified as

$$J_i = -l_{12}\nabla \ln T - l_{22}\nabla \mu_{iT}$$

$$= -l_{12}\nabla \ln T - l_{22}RT/c_i \nabla c_i \qquad \text{(A2)}$$

Since Fick's diffusion coefficient, D_i, is given by

$$D_i = l_{22}RT/c_i \qquad \text{(A3)}$$

Equation 10 is obtained by substituting Equations A1 and A3 into Equation A2.